

# On Generalisation of Isotropic Central Difference for Higher Order Approximation of Fractional Laplacian

P.H. Lam\*, H.C. So

*Department of Electrical Engineering, City University of Hong Kong, Kowloon, Hong Kong SAR*

---

## Abstract

The study of generalising the central difference for integer order Laplacian to fractional order is discussed in this paper. Analysis shows that, in contrary to the conclusion of a previous study, difference stencils evaluated through fast Fourier transform prevents the convergence of the solution of fractional Laplacian. We propose a composite quadrature rule in order to efficiently evaluate the stencil coefficients with the required convergence rate in order to guarantee convergence of the solution. Furthermore, we propose the use of generalised higher order lattice Boltzmann method to generate stencils which can approximate fractional Laplacian with higher order convergence speed and error isotropy. We also review the formulation of the lattice Boltzmann method and discuss the explicit sparse solution formulated using Smolyak's algorithm, as well as the method for the evaluation of the Hermite polynomials for efficient generation of the higher order stencils. Numerical experiments are carried out to verify the error analysis and formulations.

*Keywords:* Finite Difference, Fractional Laplacian, Double Exponential Rule, Higher Order Approximation, Smolyak

---

## 1. Introduction

Fractional Laplacian has found important applications in modelling physics, which include low frequency approximation of the Zener fractional wave model [1, 2], fractional diffusion model for porous medium [3], diffusion reaction [4], and more can be found in the review [5]. Therefore, numerical methods for fractional Laplacian is also a hot topic.

There are many definitions of fractional Laplacian. In particular, one that is defined for non-local boundary condition needs that the function undertaking the Laplacian to be defined in everywhere including the exterior of the domain under consideration. Another definition based on the eigenvalue of a boundary problem only requires the function to be defined within the boundary. For a full review of various definitions of the fractional Laplacian and numerical solutions, refer to [5]. In this paper, we consider the Riesz type, which belongs to the former definition, where the function must be defined in the entirety of real number space. We follow a similar approach as the previous work [6], where we seek a filter with a Fourier spectrum that closely resembles that of Riesz fractional Laplacian. Surprisingly, this approach has not yet been addressed in the literature [5] even though it dates as back to 2005 [7], and perhaps much earlier.

In the previous work [6], it was concluded that evaluation of the stencil coefficients by fast Fourier transform (FFT) is sufficient to achieve second and higher convergence. However, we will show that this is not the case because the spectrum of the stencil does not converge properly, resulting in a constant error, regardless of the nodal spacing. Moreover, the numerical examples only include low number of nodes, restricting the approximation error of the solution to a much higher order. This hides the fact that the spectral property of the stencil does not converge properly. A more sophisticated approach is called for to solve for those stencil coefficients in order to guarantee convergence

---

\*Corresponding author

*Email addresses:* puiholam2-c@my.cityu.edu.hk (P.H. Lam), hcso@ee.cityu.edu.hk (H.C. So)

order of the solution. Other than addressing this issue, we have made a number of improvements to it by incorporating the generalised lattice Boltzmann method. However, we do not discuss the application of this stencil in dynamic problems as it has already been addressed in [6] and many other papers.

The paper is organised as follows. First, we define notations vital for understanding of the mathematical expressions in this paper in Subsection 1.1. In Section 2, we review the generalised lattice Boltzmann method in details with additional work of our own. In Section 3, we discuss how the lattice Boltzmann method can be generalised to fractional order for approximating the fractional Laplacian. Error analysis and convergence guarantee of various methods incorporated are presented. In Section 4, we demonstrate that, in practice, the use of FFT for obtaining stencils may prevent the convergence of the solution and that our solution successfully averts this issue. And finally in the conclusion, we remark on the applied methods and suggest future study.

We would also like to highlight the contributions of this paper as follows:

- Solution and rule set for automatic generation of central difference with arbitrary order of convergence and error isotropy
- Error analysis of the generalised lattice Boltzmann is presented using the multinomial formula for understanding of the relationship between the convergence and error isotropy order with the order of Hermite quadrature
- Explicit solutions, in terms of Lagrange polynomials, for sparse multidimensional lattice Boltzmann stencils using modified Smolyak method
- More efficient method of computing the Hermite polynomials required for higher order stencil compared to [8]
- Convergence analysis of the tanh-sinh rule for inverse discrete-time Fourier transform (DTFT)
- Convergence analysis of generalised Filon method to ensure that the fractional central difference converges at a rate required for the convergence of the solution at expected rate

### 1.1. Notations

Here, we define the commonly used notations throughout the paper. Tensors are denoted by bold italic characters, and an element of an  $n$  rank tensor is denoted by a tensor with a superscript of a vector consisting of  $n$  elements. For example, indexing of the tensor  $\mathbf{T}$  with the vector indices  $\mathbf{a}$  is  $\mathbf{T}^{\mathbf{a}}$ . The number of dimensions is denoted by  $d$ . We use the probabilist's definition of Hermite polynomials given by

$$H_n = (-1)^n e^{\frac{x^2}{2}} \frac{d^n}{dx^n} e^{-\frac{x^2}{2}}. \quad (1.1)$$

The  $n$  rank Hermite tensor of dimension  $d^n$  in the Cartesian coordinate system is defined as

$$\mathbf{H}_n^{\mathbf{a}}(\mathbf{x}) = \prod_{k=0}^{d-1} H_{s(\mathbf{a}|k)}(\mathbf{x}_k), \quad (1.2)$$

where  $\mathbf{a}$  is a vector which consists of  $n$  integer indices for  $0 \leq \mathbf{a}_j < d$ , and the parity function  $s(\cdot)$  is defined as

$$s(\mathbf{a}|k) = \sum_{j=0}^{n-1} \delta_{\mathbf{a}_j, k}. \quad (1.3)$$

We also use the vector subscript on a function to define the order of derivative applied for each respective dimension of the vector

$$\left\{ \frac{\partial^{\otimes n}}{\partial \mathbf{x}^{\otimes n}} f(\mathbf{x}) \right\}^{\mathbf{a}} = f_{s(\mathbf{a})}(\mathbf{x}), \quad (1.4)$$

where  $\{\mathbf{s}(\mathbf{a})\}_k = s(\mathbf{a}|k)$ . The Laplacian operator is defined by the symbol  $\Delta$ , and the higher order Laplacian is defined as

$$\Delta^m f(\mathbf{x}) = \left( \sum_{k=0}^{d-1} \frac{\partial^2}{\partial \mathbf{x}_k^2} \right)^m f(\mathbf{x}). \quad (1.5)$$

Moreover, we define the fractional Laplacian of  $f$  as

$$-(-\Delta)^{\frac{\alpha}{2}} f(\mathbf{x}) = -\mathcal{F}^{-1} \{ |\mathbf{k}|^\alpha \mathcal{F} \{ f \}(\mathbf{k}) \}(\mathbf{x}), \quad (1.6)$$

where  $\mathcal{F}$  is the Fourier transform operator.

## 2. Central Difference based on Hermite Polynomials with Higher Order Isotropy

First we review the derivation of lattice Boltzmann method in the form of a central difference operator to approximate an arbitrary order of derivative. The difference operator  $\mathbf{D}_n$  of order  $n$  in the lattice Boltzmann method is defined by the  $d$  rank tensor contraction [9]

$$f_{\mathbf{s}(\mathbf{a})}(\mathbf{x}) \sim \mathbf{D}_n^{\mathbf{a}} \cdot \mathbf{F} = \left( \frac{a}{h} \right)^n \sum_{\substack{\mathbf{i}_j \in \{-N_h, \dots, N_h\}, \\ j=0, \dots, d-1}} w_{\mathbf{i}}^{N_q} \mathbf{H}_n^{\mathbf{a}}(\mathbf{v}_{\mathbf{i}}) f(\mathbf{x} + \mathbf{x}_{\mathbf{i}}), \quad (2.1)$$

where  $\mathbf{x}_{\mathbf{i}} = \mathbf{i}h$  are the grid points with equal spatial distance  $h$ ,  $\mathbf{v}_{\mathbf{i}} = \mathbf{a}\mathbf{i}$  are the grid points scaled by a constant factor  $a > 0$ , and  $w_{\mathbf{i}}^{N_q}$  are quadrature weights at the grid points. These weights are invariant in the sense that they are the same when swapping indices, and they satisfy the norm preservation of the continuous counterpart of inner products of Hermite polynomials, for all  $n \leq N_q$  and unique combinations of  $\mathbf{a}$  such that  $\sum_k \mathbf{a}_k = n$  with each  $\mathbf{a}_k \geq \mathbf{a}_{k+1}$ , as such

$$\sum_{\mathbf{i} \in \Omega} w_{\mathbf{i}}^{N_q} (\mathbf{H}_n^{\mathbf{a}}(\mathbf{v}_{\mathbf{i}}))^2 = \int_{\mathbb{R}^d} \prod_{k=0}^{d-1} H_{s(\mathbf{a}|k)}^2(\mathbf{x}_k) \omega(\mathbf{x}_k) \, d\mathbf{x}, \quad (2.2)$$

where  $\Omega$  is the space of indices for non-zero weights to simplify the multi-index summation, and  $\omega(x) = \frac{1}{\sqrt{2\pi}} e^{-\frac{x^2}{2}}$  is the Hermite weight function. The purpose of the scaling factor  $a$ , and the number of weights per dimension  $N_h$  required will be discussed later in Subsection 2.2.

If the weights satisfy these norm preservation conditions, they also satisfy the orthogonality conditions for inner products of Hermite polynomials. To understand how, first, consider the 1D weights, due to symmetry of the weights, when the inner product consists of polynomials of different parities, the integrand is odd, and they cancel each other from the summation of positive and negative sides. When the parities are the same but the polynomials are not of the same order, the integrand is a polynomial consisting of only monomials of even degrees. These monomials can be written as a linear combination of each of the squared polynomials because one can show that the lower triangle matrix formed from writing the squared polynomials as linear combinations of the monomials has a non-zero determinant. In fact, the inverse is given explicitly given by (14) in [10]. Since each integral of each of these squared polynomials is exactly equal to the discrete sum, the integral of the linear combinations will also yield the same result. Therefore, the discrete sum also satisfies the orthogonality of the continuous counterpart. In the multidimensional case, because the integrand is simply a product of the 1D squared polynomials in each dimension, satisfying all combinations of which the total order is lower or equal to  $N_q$  is enough. Moreover, since the weights are invariant, permutations of the orders of the polynomial in each dimension lead to the same sum, that is, the sum is also invariant. Therefore, we only need to satisfy unique combinations of degree numbers which sum to  $\leq N_q$ , regardless of the permutation.

To understand the motivation of this approximation, first, we suppose  $N_q \rightarrow \infty$  so that (2.1) can be rewritten as

$$\mathbf{D}_n^{\mathbf{a}} \cdot \mathbf{F} = \left(\frac{a}{h}\right)^n \int_{\mathbb{R}^d} \mathbf{H}_n^{\mathbf{a}}(\mathbf{v}) \omega(\mathbf{v}) f\left(\mathbf{x} - \frac{h}{a}\mathbf{v}\right) d\mathbf{v} \quad (2.3)$$

$$= \left(-\frac{a}{h}\right)^n \int_{\mathbb{R}^d} \prod_{k=0}^{d-1} \left(\frac{d^{s(\mathbf{a}|k)}}{d\mathbf{v}_k^{s(\mathbf{a}|k)}} e^{-\frac{v_k^2}{2}}\right) f\left(\mathbf{x} - \frac{h}{a}\mathbf{v}\right) d\mathbf{v} \quad (2.4)$$

$$= \int_{\mathbb{R}^d} e^{-\frac{v_k^2}{2}} \left\{ \frac{\partial^{\otimes n}}{\partial \boldsymbol{\xi}^{\otimes n}} f(\boldsymbol{\xi}) \right\} \Big|_{\boldsymbol{\xi}=\mathbf{x}-\frac{h}{a}\mathbf{v}} d\mathbf{v} \quad (2.5)$$

$$= \mathcal{F}^{-1} \left\{ e^{-\frac{1}{2} \|\frac{h}{a}\mathbf{k}\|^2} \prod_{k=0}^{d-1} (i\mathbf{k}_k)^{s(\mathbf{a}|k)} \mathcal{F}\{f\}(\mathbf{k}) \right\}(\mathbf{x}), \quad (2.6)$$

where we have assumed that  $f$  converges everywhere when expanded as a Taylor's series about any point  $\mathbf{x}$  and that  $f$  vanishes in the infinity when multiplied by the Gaussian function. This shows that the approximation is the derivative of  $f$  spectrally low-pass filtered by a Gaussian function. Expanding the Gaussian function about 0 leads to

$$\mathbf{D}_n^{\mathbf{a}} \cdot \mathbf{F} = \sum_{k=0}^{\infty} \frac{1}{2^k k!} \left(\frac{h}{a}\right)^{2k} \Delta^k f_{s(\mathbf{a})}(\mathbf{x}), \quad (2.7)$$

which shows that the operator gives the second order approximation of the derivative, with infinite order of error isotropy.

We can show that a finite  $N_q$  truncates this series to  $k = N_q - n$ , provided that  $N_q \geq n$ , with higher order terms being unknown, and thus the approximation can still be second order accurate, and the error can still be isotropic up to order  $2(N_q - n)$ . Substituting the Taylor's series expansion of  $f$  about  $\mathbf{x}$ , expressed in the multinomial form, into (2.1) gives

$$\mathbf{D}_n^{\mathbf{a}} \cdot \mathbf{F} = \left(\frac{a}{h}\right)^n \sum_{m=0}^{2N_q-n} \frac{1}{m!} \int_{\mathbb{R}^d} \left( \prod_{k=0}^{d-1} H_{s(\mathbf{a}|k)}(\mathbf{v}_k) \right) \left( \sum_{k=0}^{d-1} \frac{h}{a} \mathbf{v}_k \frac{\partial}{\partial \mathbf{x}_k} \right)^m f(\mathbf{x}) d\mathbf{v} + O(h^{2N_q-n+1}) \quad (2.8)$$

$$\sim \left(\frac{a}{h}\right)^n \sum_{m=0}^{2N_q-n} \left(\frac{h}{a}\right)^m \sum_{\sum_{k=0}^{d-1} \mathbf{b}_k = m} \frac{f_{\mathbf{b}}(\mathbf{x})}{(2\pi)^{\frac{d}{2}}} \prod_{k=0}^{d-1} \int_{-\infty}^{\infty} \frac{\mathbf{v}_k^{\mathbf{b}_k}}{\mathbf{b}_k!} H_{s(\mathbf{a}|k)}(\mathbf{v}_k) \omega(\mathbf{v}_k) d\mathbf{v}_k, \quad (2.9)$$

where the summation limits refers to all possible combinations of  $\mathbf{b}$  which satisfy the condition. The integral is only non-zero when  $\mathbf{b}_k - s(\mathbf{a}|k)$ , and thus  $m - n$ , is even and non-negative. This leaves us with only the combinations of the squared terms. Moreover, the integral with respect to each dimension results in  $2^{-l}/l!$ , where  $l = (\mathbf{b}_k - s(\mathbf{a}|k))/2$ . Therefore, we can rewrite the difference as

$$\mathbf{D}_n^{\mathbf{a}} \cdot \mathbf{F} = \sum_{m=0}^{N_q-n} \frac{1}{2^m m!} \left(\frac{h}{a}\right)^{2m} \sum_{\sum_{k=0}^{d-1} \mathbf{b}_k = m} \prod_{k=0}^{d-1} \frac{m!}{\mathbf{b}_k!} \frac{\partial^{2\mathbf{b}_k}}{\partial \mathbf{x}_k^{2\mathbf{b}_k}} f_{s(\mathbf{a})}(\mathbf{x}) + O(h^{2(N_q-n+1)}) \quad (2.10)$$

$$= \left( 1 + \sum_{m=1}^{N_q-n} \frac{1}{2^m m!} \left(\frac{h}{a}\right)^{2m} \left( \sum_{k=0}^{d-1} \frac{\partial^2}{\partial \mathbf{x}_k^2} \right)^m \right) f_{s(\mathbf{a})}(\mathbf{x}) + O(h^{2(N_q-n+1)}), \quad (2.11)$$

which is basically (2.7) but with terms higher order than  $N_q - n$  being unknowns. This shows that as long as  $N_q \geq n$ , the error is second order. However, it is only isotropic up to order  $2(N_q - n)$ , for  $N_q > n$ .

### 2.1. Higher Order Approximation

Because of the unique properties of the Taylor's series coefficients of the Gaussian function, the higher order accurate difference stencils can in fact be explicitly expressed in terms of the quadrature weights and higher order

Hermite polynomials. Here we show that an arbitrary order  $2N_c$  accurate difference method is given by

$$\mathbf{D}_n^{\mathbf{a}} \cdot \mathbf{F} = \left(\frac{a}{h}\right)^n \sum_{\mathbf{i} \in \Omega} w_{\mathbf{i}}^{N_q} \sum_{j=0}^{N_c-1} \frac{(-1)^j}{2^j j!} \mathbf{H}_{n,j}^{\mathbf{a}}(\mathbf{v}_{\mathbf{i}}), \quad (2.12)$$

$$= f_{s(\mathbf{a})}(\mathbf{x}) + O(h^{2N_c}), \quad (2.13)$$

where  $N_c$  satisfies  $N_q \geq n + 2(N_c - 1)$ , and we define the Laplacian Hermite polynomials as

$$\mathbf{H}_{n,j}^{\mathbf{a}}(\mathbf{x}) = (-1)^n e^{\sum_{k=0}^{d-1} \frac{x_k^2}{2}} \Delta^j \prod_{k=0}^{d-1} \frac{d^{\mathbf{a}_k}}{d\mathbf{x}_k^{\mathbf{a}_k}} e^{-\frac{x_k^2}{2}}. \quad (2.14)$$

From (2.11), we deduce that (2.12) leads to

$$\begin{aligned} \mathbf{D}_n^{\mathbf{a}} \cdot \mathbf{F} &= \sum_{k=0}^{N_c-1} \left( \sum_{l=0}^k \frac{1}{2^l l!} \frac{(-1)^{k-l}}{2^{k-l} (k-l)!} \right) \left(\frac{h}{a}\right)^{2k} \Delta^k f_{s(\mathbf{a})}(\mathbf{x}) \\ &\quad + \sum_{k=N_c}^{N_q-n-N_c+1} \left( \sum_{l=0}^{N_c-1} \frac{(-1)^l}{2^l l!} \frac{1}{2^{k-l} (k-l)!} \right) \left(\frac{h}{a}\right)^{2k} \Delta^k f_{s(\mathbf{a})}(\mathbf{x}) + O(h^{2(N_q-n-N_c+2)}). \end{aligned} \quad (2.15)$$

The coefficient for  $k < N_c$  can be simplified as

$$\sum_{l=0}^k \frac{1}{2^l l!} \frac{(-1)^{k-l}}{2^{k-l} (k-l)!} = \frac{(-1)^k}{2^k k!} \sum_{l=0}^k \frac{(-1)^l l!}{l! (k-l)!} \quad (2.16)$$

$$= \frac{(-1)^k}{2^k k!} \sum_{l=0}^k \binom{k}{l} (-1)^l x^{k-l} \Big|_{x=1} \quad (2.17)$$

$$= \frac{(-1)^k}{2^k k!} (x-1)^k \Big|_{x=1} = 0. \quad (2.18)$$

This proves that the error terms of order lower than  $2N_c$  are cancelled out, provided that  $N_q$  is sufficiently large. The order of isotropy of the error follows from before, and it requires  $N_q$  to satisfy  $N_q \geq 2N_c + n - 1$  for at least an error term to be isotropic.

## 2.2. 1D Grid Quadrature Problem for Hermite Weight Function

Recall that the lattice Boltzmann method has turned the derivative problem into an integral problem where we need to find coefficients such that (2.2) is satisfied. In the literature, these weights are commonly solved in the implicit matrix form [9]. We shall review the formulation of this problem in 1D and higher dimensions. Moreover, we show that the solution can be explicitly expressed in terms of Lagrange polynomials.

In 1D, this problem is straightforward to formulate as we can simply choose consecutive nodes on the grid so that the degree of freedom matches the number of conditions to satisfy. Because the squared Hermite polynomials are symmetric, the weights are also symmetric by Sobolev's invariant theorem [11]. Therefore, the weights on the negative side, in fact, do not contribute to the degree of freedom. Then, in matrix form, the linear system of equations consisting of (2.2) for various  $n$  is written as

$$\begin{bmatrix} H_0^2(0) & H_0^2(a) & \cdots & H_0^2(N_q a) \\ H_1^2(0) & H_1^2(a) & \cdots & H_1^2(N_q a) \\ \vdots & \vdots & \ddots & \vdots \\ H_{N_q}^2(0) & H_{N_q}^2(a) & \cdots & H_{N_q}^2(N_q a) \end{bmatrix} \begin{bmatrix} 1 & 0 & \cdots & 0 \\ 0 & 2 & \cdots & 0 \\ \vdots & \vdots & \ddots & \vdots \\ 0 & \cdots & 0 & 2 \end{bmatrix} \begin{bmatrix} w_0 \\ w_1 \\ \vdots \\ w_{N_q} \end{bmatrix} = \begin{bmatrix} 0! \\ 1! \\ \vdots \\ N_q! \end{bmatrix}. \quad (2.19)$$

Alternatively, one can also express this in terms of monomials and the Hermite moments as

$$\begin{bmatrix} 1 & 1 & \cdots & 1 \\ 0 & a^2 & \cdots & (N_q a)^2 \\ \vdots & \vdots & \ddots & \vdots \\ 0 & (a)^{2N_q} & \cdots & (N_q a)^{2N_q} \end{bmatrix} \begin{bmatrix} 1 & 0 & \cdots & 0 \\ 0 & 2 & \cdots & 0 \\ \vdots & \vdots & \ddots & \vdots \\ 0 & \cdots & 0 & 2 \end{bmatrix} \begin{bmatrix} w_0 \\ w_1 \\ \vdots \\ w_{N_q} \end{bmatrix} = \begin{bmatrix} 1 \\ \frac{2!}{2(1!)} \\ \vdots \\ \frac{(2N_q)!}{2^{N_q} N_q!} \end{bmatrix}. \quad (2.20)$$

The right hand side is the so-called double factorial. Solving this formulation is less stable but save on costs of computing the polynomials. With the extra variable  $a$ , one of the weights can be eliminated. Ideally, one would want the weight eliminated to be the furthest weight from the centre but this is not always possible. Numerical solutions suggest that  $w_{N_q}$  can only be eliminated for even  $N_q$ . Therefore, for the rest of the paper, we follow this conjecture. However, solving for  $a$  in the implicit form is although possible, it is likely expensive. Here, we show that it can be reduced into a root finding problem by explicitly expressing the weights in terms of the Hermite polynomials.

To formulate the explicit solution, note that the squared Hermite polynomials can be interpolated exactly by  $2N_q + 1$  points Lagrange polynomials. The integral itself can be evaluated exactly using Gauss quadrature with  $N_q + 1$  points. Therefore, the right hand side of (2.2) can be rewritten as

$$\sum_{k=-N_q}^{N_q} H_n^2(ak) \sum_{i=0}^{N_q} q_i l_k^{N_q} \left( \frac{\xi_i}{a} \right), \quad (2.21)$$

where  $q_i$  and  $\xi_i$  are the Gauss-Hermite quadrature weights and abscissae respectively, and each  $l_k^n$  is the  $2n + 1$  symmetric grid point Lagrange polynomial basis defined as

$$l_k^n(x) = \prod_{\substack{j=-n \\ j \neq k}}^n \frac{x-j}{k-j}. \quad (2.22)$$

Comparing the left and right hand sides, we see that

$$w_k = \sum_{i=0}^{N_q} q_i l_k^{N_q} \left( \frac{\xi_i}{a} \right). \quad (2.23)$$

The Gaussian weights and abscissa are most easily obtained by solving the eigenvalue problem for the tridiagonal matrix of dimension  $\mathbb{R}^{N_q \times N_q}$  given by [12]

$$\begin{bmatrix} 0 & 1 & & & & \\ 1 & 0 & \sqrt{2} & & & \\ & \sqrt{2} & \ddots & \ddots & & \\ & & \ddots & \ddots & \ddots & \\ & & & \sqrt{N_q-1} & \sqrt{N_q-1} & \\ & & & & 0 & \end{bmatrix}. \quad (2.24)$$

The diagonal elements are obtained from the recurrence relationship of the Hermite polynomials. The eigenvalues are the roots of  $H_{N_q+1}$  and thus Gauss quadrature abscissae, and the weights are given by  $v_k^2$ , where  $v_k$  is the first element of the eigenvector corresponding to the  $k$ -th eigenvalue. Again, Sobolev's theorem ensures that these weights and abscissae are symmetric, so that  $q_i = q_{N_q-i}$ , and  $\xi_i = \xi_{N_q-i}$ . Moreover, since  $l_{N_q}(x) = l_{-N_q}(-x)$ , one can rewrite the linear system of (2.21) in matrix form, similarly as (2.19). The cancellation of the matrix consisting of the Hermite polynomials on both sides confirms that (2.23) is indeed the solution of (2.19). This also validates the requirement of  $2N_q + 1$  symmetric nodes even though there are only  $N_q + 1$  conditions to satisfy, which makes it appears to require only  $N_q + 1$  weights.

With the closed-form solution, the scaling constant  $a$  can be solved by setting  $w_k^{N_q} = 0$ , resulting in the root finding problem of solving for  $a$  such that

$$\sum_{i=0}^{N_q} q_i \xi_i (\xi_i + ak) \prod_{\substack{j=1 \\ j \neq k}}^{N_q} \left( \frac{\xi_i^2}{j^2} - a^2 \right) = 0. \quad (2.25)$$

Using the symmetry of the quadrature weights and abscissae and  $\xi_{N_q/2} = 0$  for even  $N_q$ , the problem can be reduced to

$$\sum_{i=0}^{\lfloor \frac{N_q}{2} \rfloor - 1} q_i \prod_{\substack{j=0 \\ j \neq k}}^{N_q} (\xi_i^2 - a^2 j^2) = 0. \quad (2.26)$$

Alternatively, one can obtain the polynomial monomial integer coefficients first by convolution and evaluating the moments, resulting in

$$\sum_{i=1}^{N_q} c_i (a^2)^{i-1} = 0, \quad (2.27)$$

where  $c_i = \frac{(2i)!}{2^i i!} \mathcal{F}^{-1} \left\{ \prod_{j=1, j \neq k}^{N_q} (1 - j^2 e^{-i\omega}) \right\} (i-1)$ . It is not exactly known whether there is a positive real solution for  $a$  when  $k = N_q$ , other than the aforementioned conjecture when  $N_q$  is even, but one can show that when  $w_n^n = 0$ ,  $w_m^{n-1} = w_m^n$  for  $m = 0, \dots, n-1$ . In fact, one can also show that all those conditions for various  $m$  are equivalent to (2.26) when  $k = n$ . Therefore, (2.26) is the only condition we have to solve when seeking an appropriate  $a$  for the elimination of the last coefficient.

### 2.3. Multidimensional Quadrature Problem

In the multidimensional case, one can easily show that the tensor product of quadrature weights satisfy (2.2) since each dimension can be separated by multiplication. However, from (2.8), it is understood that the quadrature rule only needs to satisfy the exactness of the integral over a homogeneous polynomial of degree  $N_q$ . That is the maximum of the sum of monomial orders of all dimensions only equals  $N_q$ , but not  $dN_q$ . Although the tensor product of quadrature weights satisfies all the terms in a monomial tensor, it is dense and contains many more coefficients than necessary. This is commonly referred to as curse of dimensionality, and it can accumulate errors from the additional summations. To solve this problem, the Smolyak's method can be applied to produce sparse weights which satisfy the orthogonality requirement stated by (2.2) [13]. Before we discuss the explicit solution obtained from Smolyak's method, let us discuss the implicit solution.

From (2.2), the number of conditions is given by the triangle number  $\left( \left( 2 + \lfloor \frac{N_q}{2} \rfloor \right) \left( 1 + \lfloor \frac{N_q}{2} \rfloor \right) + \left( \lfloor \frac{N_q}{2} \rfloor + 1 \right) \lfloor \frac{N_q}{2} \rfloor \right) / 2$  in 2D. The triangle number requires that the grid spans at least  $N_q$  number of nodes on each side, the same as the 1D case. Recall that each coefficient  $w_{i,j}$  equals  $w_{j,i}$  because of the invariance theorem. Thus, we choose only nodes from a right triangle formed by  $\frac{N_q^2}{2}$  positive nodes. Further halving this right triangle as an isosceles triangle results in this triangle number of nodes. The nodes on the axes and the diagonal nodes only repeat 4 times while the nodes in between are repeated 8 times. Therefore, prioritizing nodes on the axes and diagonals results in fewer nodes. This requires shifting the nodes in the other half of the isosceles triangle towards the diagonal axis. For the nodes to be more evenly spread out, we adopt the following rule:  $w_{i,j}$  are non-zero for  $i = 0, \dots, \lfloor \frac{N_q}{2} \rfloor$ ,  $j = 0, \dots, i$ , and for  $i = \lfloor \frac{N_q}{2} \rfloor + 1, \dots, N_q$ ,  $j = 0, \lfloor \frac{i}{N_q - i} \rfloor, \lfloor \frac{2i}{N_q - i} \rfloor, \dots$ . This gives us the most optimised scheme for the 2D case.

For example, for the case  $N_q = 4$ , we have the following set of nodes  $\mathbf{i} \in \{(0, 0), (1, 0), (1, 1), (2, 0), (2, 1), (2, 2),$

$(3, 0), (3, 3), (4, 0)$ . The orthogonality conditions to satisfy are then

$$\begin{bmatrix} (H_4(0)H_0(0))^2 & (H_4(a)H_0(0))^2 & \cdots & (H_4(3a)H_0(3a))^2 & (H_4(2a)H_0(a))^2 \\ (H_3(0)H_1(0))^2 & (H_3(a)H_1(0))^2 & \cdots & (H_3(3a)H_1(3a))^2 & (H_3(2a)H_1(a))^2 \\ (H_3(0)H_0(0))^2 & & & & \\ (H_2(0)H_2(0))^2 & & & & \\ (H_2(0)H_1(0))^2 & \vdots & & \vdots & \vdots \\ (H_2(0)H_0(0))^2 & & & & \\ (H_1(0)H_1(0))^2 & & & & \\ (H_1(0)H_0(0))^2 & & & & \\ (H_0(0)H_0(0))^2 & (H_0(a)H_0(0))^2 & \cdots & (H_0(3a)H_0(3a))^2 & (H_0(2a)H_0(a))^2 \end{bmatrix} \begin{bmatrix} 8 & 0 & \cdots & 0 \\ 0 & 4 & & 0 \\ \vdots & & \ddots & \vdots \\ 0 & 0 & \cdots & 1 \end{bmatrix} = \begin{bmatrix} w_{0,0} \\ w_{1,0} \\ w_{2,0} \\ w_{3,0} \\ w_{4,0} \\ w_{1,1} \\ w_{2,2} \\ w_{3,3} \\ w_{2,1} \end{bmatrix} = \begin{bmatrix} 4!0! \\ 3!1! \\ 3!0! \\ 2!2! \\ 2!1! \\ 2!0! \\ 1!1! \\ 1!0! \\ 0!0! \end{bmatrix}. \quad (2.28)$$

Solving the inverse problem for (2.28) gives us the 2D grid quadrature weights. As with the 1D case, the furthest node from the centre can be eliminated by choosing the appropriate grid spacing multiplier for even  $N_q$ . In the above example,  $w_{4,0}$  shall be 0. This is one of the reasons that the last node on the last row has not been shifted to the diagonal. We shall also see that the weight of this node is equal to that of the furthest node in the 1D case in the explicit solution. Indeed, solving (2.26) gives us the multiplier required to eliminate that node on the edge.

To derive the modified Smolyak's method, we start from the fundamentals of Smolyak's method. It is derived by first rewriting the 1D weights as a telescoping sum as follows

$$\mathbf{w}_{N_q} = \mathbf{w}_0 + \sum_{k=1}^{N_q} \mathbf{w}_k - \mathbf{w}_{k-1}. \quad (2.29)$$

One can show that summing the tensor products of the weights of arbitrary dimension  $\mathbf{W}_{N_q-k}$  and differences of 1D weights of order  $k$ , mathematically expressed as

$$\mathbf{W}_{N_q}^{d+1} = \mathbf{W}_{N_q}^d \otimes \mathbf{w}_0 + \sum_{k=1}^{N_q} \mathbf{W}_{N_q-k}^d \otimes (\mathbf{w}_k - \mathbf{w}_{k-1}), \quad (2.30)$$

results in a set of higher rank weights which satisfy the monomial degree exactness requirement. To see this, first notice that given the monomial order of the new dimension  $n$ , the weighted sum of the monomial from the difference terms for  $k > n$  are zero because the two sets of weights both lead to exact evaluation of the integral. For  $k \leq n$ , since the sum of the monomial degrees for the rest of the dimensions is equal to  $N_q - n$ , the weighted sum is the following telescoping sum,

$$\mathbf{W}_{N_q}^{d+1} \cdot \chi_{N_q} = \left( \mathbf{W}_{N_q-n}^d \cdot \mathbf{X}_{N_q-n}^d \right) \otimes \left( (\mathbf{w}_n \cdot \mathbf{x}^n) + \sum_{k=0}^{n-1} (\mathbf{w}_k - \mathbf{w}_k) \cdot \mathbf{x}^n \right) \quad (2.31)$$

$$= \left( \mathbf{W}_{N_q-n}^d \cdot \mathbf{X}_{N_q-n}^d \right) \otimes (\mathbf{w}_n \cdot \mathbf{x}^n), \quad (2.32)$$

where  $\chi$  is the  $d+1$  rank monomial tensor of order  $N_q$ ,  $\mathbf{X}_{N_q-n}$  is the  $d$  rank monomial tensor of order  $N_q - n$ , and the weights in the weighted sum of  $\mathbf{X}_{N_q-n}$  are all replaced with the lowest order  $N_q - n$  because the monomial order is smaller than or equal to that of the weights. This evaluates exactly to the moment as all the monomial orders are matched with the weights.

For the 2D case, setting the weights  $\mathbf{w}_k$  for both the differences and the weights on the left side of the tensor product in (2.30) to 1D weights with  $2k+1$  consecutive nodes as in (2.23) results in 2D weights positioned in an isosceles triangle on the grid. Attempting to position the nodes towards the diagonal by setting the Lagrange interpolation nodes to be at  $j=0, \left\lfloor \frac{k}{N_q-k} \right\rfloor, \left\lfloor \frac{2k}{N_q-k} \right\rfloor, \dots$  for each  $\mathbf{w}_k$  where  $k \leq \left\lfloor \frac{N_q}{2} \right\rfloor$  in (2.30) leads to denser rows/columns towards the edge. The trick to eliminate the weights in the in-between nodes is to modify the Smolyak method to use a linear





Because of the asymmetry, the zero conditions for both the column and the row need to be satisfied in order to satisfy the condition for where the non-zero weights are, set out in (2.28) for instance. While this formulation seems asymmetric in the written form, it still satisfies the exactness condition given by (2.31), and thus the orthogonality condition. Because the solution which satisfies all the conditions is unique, the final weighted sum shall become symmetric again. Enforcing the condition for both elements to be zero, we arrive at the linear system

$$\begin{aligned} & \begin{bmatrix} \left\{ \mathbf{w}_{\lceil \frac{N_q}{2} \rceil} \right\}_{\bar{\mathbf{i}}_0} \left\{ \mathbf{w}_{\lfloor \frac{N_q}{2} \rfloor, \mathbf{i}_0} \right\}_{\lceil \frac{N_q}{2} \rceil} & 0 \\ 0 & \left\{ \mathbf{w}_{\lceil \frac{N_q}{2} \rceil} - \mathbf{w}_{\lfloor \frac{N_q}{2} \rfloor, \mathbf{i}_0} \right\}_{\lceil \frac{N_q}{2} \rceil} \left\{ \mathbf{w}_{\lfloor \frac{N_q}{2} \rfloor, \mathbf{i}_1} \right\}_{\bar{\mathbf{i}}_0} \end{bmatrix} \begin{bmatrix} b_0 \\ b_1 \end{bmatrix} \\ & = - \left( \begin{bmatrix} 0 & \left\{ \mathbf{w}_{\lfloor \frac{N_q}{2} \rfloor, \mathbf{i}_0} \right\}_{\lceil \frac{N_q}{2} \rceil} \left\{ \mathbf{w}_{\lceil \frac{N_q}{2} \rceil} \right\}_{\bar{\mathbf{i}}_0} \\ \left\{ \mathbf{w}_{\lfloor \frac{N_q}{2} \rfloor, \mathbf{i}_0} \right\}_{\lceil \frac{N_q}{2} \rceil} \left\{ \mathbf{w}_{\lceil \frac{N_q}{2} \rceil} \right\}_{\bar{\mathbf{i}}_0} \end{bmatrix} + \begin{bmatrix} \left\{ \bar{\mathbf{w}}_{\lfloor \frac{N_q}{2} \rfloor} \right\}_{\bar{\mathbf{i}}_0, \lceil \frac{N_q}{2} \rceil} \\ \left\{ \bar{\mathbf{w}}_{\lceil \frac{N_q}{2} \rceil} \right\}_{\bar{\mathbf{i}}_0, \lfloor \frac{N_q}{2} \rfloor} \end{bmatrix} \right), \quad (2.38) \end{aligned}$$

where, the last set of unknown weights are given by  $\bar{\mathbf{w}}_{\lfloor \frac{N_q}{2} \rfloor} = \mathbf{w}_{\lfloor \frac{N_q}{2} \rfloor, \mathbf{i}_0} b_0 + \mathbf{w}_{\lfloor \frac{N_q}{2} \rfloor, \mathbf{i}_1} b_1$ . This again has a trivial solution, which can be used to complete (2.33).

#### 2.4. Evaluation of Hermite Polynomials

It is well known that the Hermite polynomials can be evaluated through the recurrence relationship

$$H_{n+1} = xH_n - nH_{n-1}. \quad (2.39)$$

These can be multiplied together through (1.2) to form the Hermite polynomial tensor. The higher order difference method stated by (2.12) calls for the evaluation of the multinomial of Hermite polynomials. This involves many terms but there is a much more efficient method to evaluate it because of the isotropy of the Gaussian function. If we show that the Laplacian Hermite polynomials with  $n = 0$  and  $n = 1$  satisfy the following relationships

$$H_{0,m}(\mathbf{x}) = rH_{1,m-1}(\mathbf{x}) - (d + 2(m - 1))H_{0,m-1}(\mathbf{x}), \quad (2.40)$$

$$H_{1,m+1}(\mathbf{x}) = rH_{0,m}(\mathbf{x}) - 2mH_{1,m-1}(\mathbf{x}), \quad (2.41)$$

$$H_{0,0}(\mathbf{x}) = 1, \quad (2.42)$$

$$H_{1,0}(\mathbf{x}) = r, \quad (2.43)$$

$$\mathbf{H}_{1,m}^{\mathbf{e}_k}(\mathbf{x}) = \frac{\mathbf{x}_k}{r} H_{1,m}(\mathbf{x}), \quad (2.44)$$

where  $r = \|\mathbf{x}\|_2$ , there is no longer the need to evaluate all the multinomial terms and combine them all to form the Laplacian. For higher  $n$ , one can continue applying the standard recurrence relationship of the Hermite polynomials, starting from (2.44). In fact, we observe that the recurrence relationship (2.41) is exactly the same as the standard recursion for the Hermite polynomial of order  $2m + 1$ .

To prove the relationships, first we define the hyperspherical coordinates for the Cartesian coordinate system of an arbitrary number of dimensions as

$$\mathbf{x}_0 = r \prod_{m=1}^{d-1} \sin \theta_k, \quad (2.45)$$

$$\mathbf{x}_k = r \cos \theta_k \prod_{m=k+1}^{d-1} \sin \theta_m, \text{ for } k = 1, \dots, d - 1. \quad (2.46)$$

Clearly, the Hermite polynomials depend only on  $r$ . Therefore, using (2.14), one can write in hyperspherical coordinates, for  $n = 0, 1$ ,

$$H_{0,m}(r) = \mathbf{e}^{\frac{r^2}{2}} \Delta^m \mathbf{e}^{-\frac{r^2}{2}}, \quad (2.47)$$

$$H_{1,m}(r) = -\mathbf{e}^{\frac{r^2}{2}} \Delta^m \frac{\partial}{\partial r} \mathbf{e}^{-\frac{r^2}{2}}, \quad (2.48)$$

where one can easily show that (2.44) is true by substituting the Jacobian matrix multiplication

$$\begin{bmatrix} \frac{\partial f}{\partial \mathbf{x}_0} \\ \frac{\partial f}{\partial \mathbf{x}_1} \\ \vdots \\ \frac{\partial f}{\partial \mathbf{x}_{d-1}} \end{bmatrix} = \begin{bmatrix} \frac{\partial r}{\partial \mathbf{x}_0} & \frac{\partial \theta_1}{\partial \mathbf{x}_0} & \cdots & \frac{\partial \theta_{d-1}}{\partial \mathbf{x}_0} \\ \frac{\partial r}{\partial \mathbf{x}_1} & \frac{\partial \theta_1}{\partial \mathbf{x}_1} & \cdots & \frac{\partial \theta_{d-1}}{\partial \mathbf{x}_1} \\ \vdots & \vdots & \ddots & \vdots \\ \frac{\partial r}{\partial \mathbf{x}_{d-1}} & \frac{\partial \theta_1}{\partial \mathbf{x}_{d-1}} & \cdots & \frac{\partial \theta_{d-1}}{\partial \mathbf{x}_{d-1}} \end{bmatrix} \begin{bmatrix} \frac{\partial f}{\partial r} \\ \frac{\partial f}{\partial \theta_1} \\ \vdots \\ \frac{\partial f}{\partial \theta_{d-1}} \end{bmatrix} \quad (2.49)$$

into (2.48). One can also show that the Laplacian of an isotropic function  $f$  is given by

$$\Delta f = \frac{1}{r^{d-1}} \frac{\partial}{\partial r} r^{d-1} \frac{\partial f}{\partial r}, \quad (2.50)$$

using the diagonal metric tensor. Then, for  $H_{0,m}$ , integrating by parts gives

$$-\frac{1}{r^{d-1}} \frac{\partial}{\partial r} r^{d-1} H_{1,m-1} = r e^{\frac{r^2}{2}} \Delta^{m-1} \frac{\partial}{\partial r} e^{-\frac{r^2}{2}} + e^{\frac{r^2}{2}} \frac{1}{r^{d-1}} \frac{\partial}{\partial r} r^{d-1} \frac{\partial}{\partial r} \Delta^{m-1} e^{-\frac{r^2}{2}} \quad (2.51)$$

$$= H_{0,m} - r H_{1,m-1}. \quad (2.52)$$

Therefore, it remains to show that  $\frac{1}{r^{d-1}} \frac{\partial}{\partial r} r^{d-1} H_{1,m-1} = (d+2(m-1)) H_{0,m-1}$ . This is equivalent to the divergence written in the Cartesian coordinate system as

$$\frac{1}{r^{d-1}} \frac{\partial}{\partial r} r^{d-1} H_{1,m-1} = - \sum_{k=0}^{d-1} \frac{\partial}{\partial \mathbf{x}_k} \left( e^{\frac{r^2}{2}} \Delta^{m-1} \frac{\partial}{\partial \mathbf{x}_k} e^{-\frac{r^2}{2}} \right), \quad (2.53)$$

$$= e^{\frac{r^2}{2}} \sum_{k=0}^{d-1} \frac{\partial}{\partial \mathbf{x}_k} \Delta^{m-1} \left( \mathbf{x}_k e^{-\frac{r^2}{2}} \right) - \mathbf{x}_k \Delta^{m-1} \frac{\partial}{\partial \mathbf{x}_k} e^{-\frac{r^2}{2}}. \quad (2.54)$$

Expanding the Laplacian in the second term, we get

$$\sum_{k=0}^{d-1} \frac{\partial}{\partial \mathbf{x}_k} \Delta^{m-1} \left( \mathbf{x}_k e^{-\frac{r^2}{2}} \right) = \sum_{k=0}^{d-1} \sum_{\sum_{j=0}^{d-1} a_j = m-1} \frac{(m-1)!}{a_k!} \frac{\partial^{2a_k+1}}{\partial \mathbf{x}_k^{2a_k+1}} \left( \mathbf{x}_k e^{-\frac{r^2}{2}} \right) \prod_{\substack{j=0 \\ j \neq k}}^{d-1} \frac{1}{a_j!} \frac{\partial^{2a_j}}{\partial \mathbf{x}_j^{2a_j}} e^{-\frac{r^2}{2}}. \quad (2.55)$$

Applying the binomial expansion to the product rule, one gets the identity

$$\frac{\partial^{2a_k+1}}{\partial \mathbf{x}_k^{2a_k+1}} \left( \mathbf{x}_k e^{-\frac{r^2}{2}} \right) = \mathbf{x}_k \frac{\partial^{2a_k+1}}{\partial \mathbf{x}_k^{2a_k+1}} e^{-\frac{r^2}{2}} + (2a_k+1) \frac{\partial^{2a_k}}{\partial \mathbf{x}_k^{2a_k}} e^{-\frac{r^2}{2}}. \quad (2.56)$$

Substituting it into (2.55) gives

$$= \sum_{\sum_{j=0}^{d-1} a_j = m-1} \left( \sum_{k=0}^{d-1} (2a_k+1) \right) \prod_{j=0}^{d-1} \frac{(m-1)!}{a_j!} \frac{\partial^{2a_j}}{\partial \mathbf{x}_j^{2a_j}} e^{-\frac{r^2}{2}} + \sum_{k=0}^{d-1} \mathbf{x}_k \Delta^{m-1} \frac{\partial}{\partial \mathbf{x}_k} e^{-\frac{r^2}{2}}, \quad (2.57)$$

$$= (2(m-1) + d) \Delta^{m-1} e^{-\frac{r^2}{2}} + \sum_{k=0}^{d-1} \mathbf{x}_k \Delta^{m-1} \frac{\partial}{\partial \mathbf{x}_k} e^{-\frac{r^2}{2}}, \quad (2.58)$$

which can be substituted back into (2.54) to prove (2.40).

For the odd case  $H_{1,m}$ , using integration by parts, we similarly have

$$\frac{\partial}{\partial r} H_{0,m} = r H_{0,m} - H_{1,m}. \quad (2.59)$$

The left hand side, again, can be expressed in the Cartesian coordinate system as

$$\frac{\partial}{\partial r} H_{0,m} = \frac{r}{\mathbf{x}_k} \frac{\partial}{\partial \mathbf{x}_k} H_{0,m} \quad (2.60)$$

$$= \frac{r}{\mathbf{x}_k} \sum_{\sum_{j=0}^{d-1} a_j = m} \frac{m!}{a_k!} \frac{\partial H_{2a_k}(\mathbf{x}_k)}{\partial \mathbf{x}_k} \prod_{\substack{j=0 \\ j \neq k}}^{d-1} \frac{H_{2a_j}(\mathbf{x}_j)}{a_j!} \quad (2.61)$$

$$= \frac{2mr}{\mathbf{x}_k} \sum_{\sum_{j=0}^{d-1} a_j = m-1} \frac{(m-1)!}{a_k!} H_{2a_k+1}(\mathbf{x}_k) \prod_{\substack{j=0 \\ j \neq k}}^{d-1} \frac{H_{2a_j}(\mathbf{x}_j)}{a_j!} \quad (2.62)$$

$$= \frac{2mr}{\mathbf{x}_k} \mathbf{H}_{1,m-1}^{\mathbf{e}_k}(\mathbf{x}) = 2m H_{1,m-1}(\mathbf{x}). \quad (2.63)$$

Therefore, (2.59) is equivalent to (2.41).

### 3. Generalisation to Fractional Order Laplacian

The error analysis in Section 2.1 gives (2.15), which states that provided that  $f$  is  $C^n$  and the  $n+2$  power of Laplacian is finite at the point of evaluation, one can evaluate its Laplacian up to  $O(h^n)$  accuracy. This result can in fact be used to generalise to fractional order Laplacian, and further to other central difference type.

Here, we propose that given a central difference stencil  $\mathbf{H}$  such that the Laplacian of a function  $f$  can be approximated by the tensor contraction as

$$\Delta f(\mathbf{x}) = h^{-2} \mathbf{H} \cdot \mathbf{F} + O(h^{2n}), \quad (3.1)$$

where  $\mathbf{F}$  consists of  $f$  evaluated at various symmetric grid points  $\mathbf{x} \pm i\mathbf{h}$ , the fractional Laplacian  $-\left(-\Delta^{\frac{\alpha}{2}}\right)f$  can be approximated as

$$-\left(-\Delta^{\frac{\alpha}{2}}\right)f = h^{-\alpha} \mathbf{H}_\alpha \cdot \mathbf{F} + O(h^{2n}), \quad (3.2)$$

where

$$\mathbf{H}_\alpha^{\mathbf{m}} = \frac{-1}{\pi^d} \int \dots \int_0^\pi \prod_{l=0}^{d-1} \cos(\mathbf{m}_l \mathbf{k}_l) \left| \sum_{\mathbf{n} \in \mathbf{H}^{\mathbf{n}} \neq 0} \mathbf{H}^{\mathbf{n}} \prod_{l=0}^{d-1} \cos(\mathbf{n}_l \mathbf{k}_l) \right|^{\frac{\alpha}{2}} d\mathbf{k}. \quad (3.3)$$

The proof can be obtained by realising that (3.1) is satisfied if and only if  $f$  is at least  $C^{2n}$ , and the discrete-time Fourier transform of the difference operator is given by

$$\mathcal{F}\{h^{-2} \mathbf{H}\}(\mathbf{k}) = h^{-2} \sum_{\mathbf{n} \in \mathbf{H}^{\mathbf{n}} \neq 0} \mathbf{H}^{\mathbf{n}} \prod_{l=0}^{d-1} \cos(\mathbf{n}_l \mathbf{k}_l) = -|\mathbf{k}|^2 \left(1 + |\mathbf{k}|^{2n} O(h^{2n})\right). \quad (3.4)$$

The fractional power of it can be expanded at the origin, using Faadi Bruno's formula, or its variants [14], as a Taylor Series as

$$\left(-\mathcal{F}\{h^{-2} \mathbf{H}\}(\mathbf{k})\right)^{\frac{\alpha}{2}} = |\mathbf{k}|^\alpha \left(1 + |\mathbf{k}|^{2n} O(\alpha^{2n} h^{2n})\right). \quad (3.5)$$

The exact coefficients can be evaluated by using FFT, which is faster than the Faadi Bruno's formula (see [15] for details). Applying inverse DTFT to the above shows that the fractional operator (3.3) is indeed also  $O(h^{2n})$ . One can also see that since the coefficients are simply convolution of coefficients of lower order terms, the order of isotropy remains the same. Therefore, the benefit of improved isotropy from the generalised lattice Boltzmann method carries over to approximating the fractional order Laplacian.

The difficulty in such technique is in evaluating the integral given by (3.3). In [6], although the fast and efficient method of FFT is applied to evaluate this integral, we shall see that it will prevent the solution from converging. Applying FFT is equivalent to applying the trapezoidal rule. Because of the branch point at the origin, the convergence of the stencil is limited to  $1 + \alpha$  for the 1D problem, which when multiplied by  $h^{-\alpha}$  gives an error of  $O(h)$  for  $2N + 1$  of the stencil coefficients about the origin. This error has been observed in the numerical experiment in [6] and seems to be  $O(h^2)$  for 2D. However, for the 1D problem, one can easily show that the second order accurate stencil, when evaluated with FFT, gives an  $O(1)$  error, meaning the spectrum of the stencil, and thus the solution will not converge with respect to the spatial distance used. Using the convolution theorem, the definition of Dirac comb function, and the closed-form solution for the stencil [15], one finds that the error of the stencil evaluated through FFT with  $2N + 1$  terms is

$$\mathbf{h}_n^\alpha - \widetilde{\mathbf{h}}_n^\alpha = - \sum_{\substack{k=-\infty \\ k \neq 0}}^{\infty} \mathbf{h}_{n+2Nk}^\alpha = \sum_{\substack{k=-\infty \\ k \neq 0}}^{\infty} (-1)^{n+1} \left( \frac{\alpha}{2} + n + 2Nk \right) > 0. \quad (3.6)$$

Then, the error in the discrete Fourier domain in the origin is

$$\text{FFT}_{2N+1} \left\{ \mathbf{h}^\alpha - \widetilde{\mathbf{h}}^\alpha \right\}_0 = \sum_{n=-N}^N \left( \mathbf{h}_n^\alpha - \widetilde{\mathbf{h}}_n^\alpha \right) > 2NhC = O(1), \quad (3.7)$$

where  $C$  is a constant. While this error is not easily generalised to other combinations of orders and dimensions, we shall see that this error is similar in other settings through numerical experiments, and it limits the convergence of the difference method at higher  $N$ .

One method to avoid the error at the origin is to apply dithering to the filter. If we can estimate the error amplitude correctly, this randomises the error and prevents patterns to show up at a specific band, such as the DC. However, we have not found a way to analyse the error pattern without significant amount of computation for the generalisation. Instead, we opt for integration techniques which allow us to evaluate this integral at higher order convergence rates greater than the expected convergence rate for solution. With the stencil error reducing faster than the solution, the convergence of the solution is no longer hindered.

### 3.1. Double Exponential Integration Rule

One strategy to avoid the branch point is to map it to infinity where the measure approaches 0, so that the main contribution of the integral is far away from that branch point. An example of this mapping is the exponential substitution. With the integrand becoming zero at the endpoints, the trapezoidal rule converges geometrically. One exponential rule is the tanh rule, which maps  $(-\infty, \infty)$  to  $(-1, 1)$ . However, its convergence is limited by the slow decay of the measure, requiring a higher number of quadrature points to cover the range. When linking the the number of quadrature points with grid distance as in [16], it has a convergence rate of  $O(e^{-C\sqrt{N}})$ . This is remedied by the double exponential substitution such as the tanh-sinh rule, which allows the integral to converge at  $O(e^{-CN/\log(N)})$ , where  $C$  is a constant [17]. Double exponential substitution has been applied to solve many integral problems involving singularity or branch points such as in [18], where the Laplace transform of  $t^\beta$  is considered.

For Fourier transform, the integrand involves an oscillatory function, but since it does not introduce any branch cut/point between the lines  $x - i\frac{\pi}{2}$  and  $x + i\frac{\pi}{2}$ , on which the poles of the tanh-sinh function are located, the convergence is not affected. However, assuming that we double the number of quadrature points for every halving of the difference nodal distance, this together with its exponential convergence still does not answer whether the evaluated stencil allows the convergence of the solution yet because we are also doubling the maximum frequency of the oscillatory function for the additional coefficients. Below, we would like to justify that given that the  $N$ -th coefficient of the 1D case of (3.3), given by

$$\mathbf{h}_N^\alpha = \frac{-1}{2\pi} \int_0^{2\pi} \cos(N\omega) \left| \sum_{n=-N_q}^{N_q} \mathbf{h}_n \cos(n\omega) \right|^{\frac{\alpha}{2}} d\omega, \quad (3.8)$$

is approximated by the tanh-sinh rule with  $N_t$  nodes on each side and with error  $e$ , then the error of the  $2N$ -th term, given by

$$\mathbf{h}_{2N}^\alpha = -\frac{x^*}{N_t} \left( \frac{\pi}{4} \left| \sum_{n=-N_q}^{N_q} (-1)^n \mathbf{h}_n \right|^{\frac{\alpha}{2}} + \sum_{k=1}^{N_t} \left| \sum_{n=-N_q}^{N_q} \mathbf{h}_n \cos \left( n \tilde{\psi} \left( \frac{x^* k}{N_t} \right) \right) \right|^{\frac{\alpha}{2}} \cos \left( 2N \tilde{\psi} \left( \frac{x^* k}{N_t} \right) \right) \psi' \left( \frac{x^* k}{N_t} \right) \right), \quad (3.9)$$

where  $\psi(x) = \tanh\left(\frac{\pi}{2} \sinh(x)\right)$ ,  $\tilde{\psi}(x) = \pi(\psi(x) + 1)$ ,  $x^*$  is the distance from the origin such that the integrand's relative magnitude to the origin is smaller than the smallest difference between two numbers allowed by the floating point precision, is at max  $O(e)$ . The symmetry allows us to only sum from one side, saving half of the computation. This grid choice as opposed to relating  $N_t$  with the grid spacing stems from the fact that  $N_t$  is much larger than the typical cases due to the oscillatory nature of the integrand. The initial guess for  $x^*$  is based on the approximation of  $\psi'$  for large  $x$  given by

$$\psi'(x) > \pi e^{-\frac{\pi}{2} e^x}. \quad (3.10)$$

The spectrum of the integer order central difference is approximated by  $4 \sin^2\left(\frac{\omega}{2}\right)$ . Then, we have approximately

$$x^* \sim \log \left( -\frac{2(\log(\epsilon) - \alpha \log(\pi))}{\pi(\alpha + 1)} \right), \quad (3.11)$$

where  $\epsilon$  is the smallest number which the floating point number can represent with the exponent being 0. The tolerance  $\epsilon$  is further divided by a factor to further account for the underestimation.

To show that the error is, at the maximum, of the same order, we apply the reproducing kernel

$$K(z, w) = \frac{\psi'(z) \overline{\psi'(w)}}{1 - \psi(z) \overline{\psi(w)}}, \quad (3.12)$$

which has been employed in [16] for the error analysis of the tanh rule, and estimate the  $H^2$  norm, with respect to the reproducing kernel, of the error operator given by

$$E^m f = \int_{-\infty}^{\infty} \cos(m\pi\psi(x)) f(x) dx - \sum_{k=-\infty}^{\infty} \cos(m\pi\psi(kh_e)) f(kh_e), \quad (3.13)$$

where  $f$  is an analytic function on the real line belonging to the reproducing kernel function space. The norm of a bounded linear operator in this space is given by [16]

$$\|E_m\|^2 = E_{(z)}^m E_{(w)}^m K(z, w). \quad (3.14)$$

The integral and the sum can be grouped together for analysis by shifting the integration domain to a line on the imaginary plane as such

$$E^m f = \Re \left\{ \int_{i\beta-\infty}^{i\beta+\infty} \phi(z) \cos(m\pi\psi(z)) f(z) dz \right\}, \quad (3.15)$$

where  $0 < \beta < \frac{\pi}{2}$ , and  $\phi(z) = \left(1 - i \cot\left(\frac{\pi}{h_e} z\right)\right)$ , and  $f$  is analytic between the lines  $x \pm i\beta$ . For small  $h_e$ ,  $\phi$  can be approximated as

$$\phi(x + i\beta) \sim -2 \exp\left(\frac{2\pi}{h_e} (ix - \beta)\right). \quad (3.16)$$

The real and imaginary parts of the cosine function are, respectively,

$$\Re \{ \cos(m\pi\psi(x + i\beta)) \} = \cos \left( \frac{\pi m \sinh(\pi \cos(\beta) \sinh(x))}{\cos(\pi \sin(\beta) \cosh(x)) + \cosh(\pi \cos(\beta) \sinh(x))} \right) \cosh \left( \frac{\pi m \sin(\pi \sin(\beta) \cosh(x))}{\cos(\pi \sin(\beta) \cosh(x)) + \cosh(\pi \cos(\beta) \sinh(x))} \right), \quad (3.17)$$

$$\Im \{ \cos(m\pi\psi(x + i\beta)) \} = - \sin \left( \frac{\pi m \sinh(\pi \cos(\beta) \sinh(x))}{\cos(\pi \sin(\beta) \cosh(x)) + \cosh(\pi \cos(\beta) \sinh(x))} \right) \cdot \sinh \left( \frac{\pi m \sin(\pi \sin(\beta) \cosh(x))}{\cos(\pi \sin(\beta) \cosh(x)) + \cosh(\pi \cos(\beta) \sinh(x))} \right). \quad (3.18)$$

Now let us consider only the amplitude and ignore the oscillatory function. The real part can be approximated as

$$\cosh \left( \frac{\pi m \sin(\pi \sin(\beta) \cosh(x))}{\cos(\pi \sin(\beta) \cosh(x)) + \cosh(\pi \cos(\beta) \sinh(x))} \right) < \frac{1}{2} \left( e^{m\pi \tan(\frac{\pi}{2} \sin \beta) e^{-\frac{\pi}{2} \cos(\beta) \left( \exp(\frac{x^2}{2}) - 1 \right)}} + 1 \right), \quad (3.19)$$

while the imaginary part can be approximated as

$$\sinh \left( \frac{\pi m \sin(\pi \sin(\beta) \cosh(x))}{\cos(\pi \sin(\beta) \cosh(x)) + \cosh(\pi \cos(\beta) \sinh(x))} \right) < e^{m\pi \tan(\frac{\pi}{2} \sin \beta) e^{-\frac{\pi}{2} \cos(\beta) \left( \exp(\frac{x^2}{2}) - 1 \right)}} - 1. \quad (3.20)$$

Since the amplitude of the kernel function behaves like the Gaussian function, when the real part is multiplied by the kernel, the integral of the offset part is integrated to a constant, which is  $O\left(e^{-\frac{C}{h_c}}\right)$  when multiplied by  $\phi$ . For the triple exponential part, which is also present in the imaginary part, it integrates to  $O\left(e^{Cm}\right)$ , where  $0 < C < 1$ , on its own. Therefore, removing the oscillatory functions from the norm integral (3.14), which is equivalent to setting them to a positive constant function, leading to an integral of product of positive Gaussian like functions, one can conclude that, regardless of  $\beta$ , the integral is  $O\left(e^{C_1 m - \frac{C_2}{h_c}}\right)$ , and so is the norm. Numerical experiment suggests that as  $m$  and  $h_c^{-1}$  become very large,  $\frac{C_2}{C_1}$  approaches 1 with  $C_2 > C_1$ . Therefore, halving of  $h$  still allows the exponential convergence of  $2m$ -th stencil coefficient. An estimate of the number of coefficients required by the trapezoidal rule can be obtained from evaluating the second order stencil, where the exact solution is known. As the analysis applies to other analytic integrands, it is also valid for higher order stencils, especially since they behave similarly.

Another issue that can prevent convergence is the limited numerical precision. When evaluating the DTFT of the integer order stencil and the tanh-sinh function near the end point  $\pm x^*$ , the relative error is much greater if the terms in (3.9) are directly evaluated. Near the end points, the cosine function needs to be evaluated to a value close to 1 and be cancelled to obtain the DTFT value, which is close to zero. However, with the floating point limited to the number of digits it can represent, the smallest non-zero DTFT value is limited to that number. If the cosine function is expressed in terms of the sine function instead, the floating point can make use of the exponent to represent a much smaller number, allowing a wider range of DTFT to be evaluated to non-zero values smaller than  $\epsilon$ . For tanh-sinh, the series expansion of  $\frac{1}{1+x}$  at infinity gives

$$\tanh\left(\frac{\pi}{2} \sinh x\right) = e^{-\pi \sinh x} - e^{-2\pi \sinh x} + e^{-3\pi \sinh x} + \dots \quad (3.21)$$

Further expansion allows us to evaluate to even smaller number, but this is not needed as the solution for  $x^*$  is around 3.28 for a constant function and double precision. The attempts to evaluate these functions more accurately only provide little improvement for coefficients far from the centre, however, because those coefficients still require cancellation of the summation terms, which are limited by the relative error given by  $\epsilon$  in (3.11).

In the 2D case, it is no longer just a branch point but there are branch cuts along both the axis, and similarly for 3D, there are branch surfaces. Applying the tanh-sinh mapping to each of variables will still map the branching to the infinity, and so the convergence is not affected. However, we do need the full tensor product, since the Smolyak algorithm to sparsify the integral operator is not applicable. This is because each dimension must reach  $N$ -th term, so we cannot mix in rules with lower number of terms.

### 3.2. Higher order Filon Method

The tanh-sinh rule clearly has a much higher computational requirement than FFT. Therefore, we propose that we specify a small number  $h_g$  away from the origin of the Fourier domain, so that the integral (3.3) is split up into two portions for each dimension, from 0 to  $h_g$ , and from  $h_g$  to  $\pi$ . The DTFT of the integer order stencil can now be expanded as a Taylor's series at  $h_g$ , and so a polynomial based grid quadrature rule can be setup to use FFT coefficients.

The quadrature rule with the sine or cosine function as the weight function and three point interpolation is termed the Filon-Simpson rule [19]. Below, we discuss the generalisation of Filon's approach to higher order so that the stencil coefficients converge at speeds required.

Evaluating the integral from 0 to  $h_g$  means that the trapezoidal summation is no longer symmetric. While this doubles the amount of coefficients to be summed, the number of cycles of the cosine functions are also reduced. This effectively means that the frequency is reduced when the mapping for the tanh-sinh rule is applied. Following the deduction from the previous subsection, the number of terms required to achieve the same error tolerance is also significantly reduced. Do note that  $h_g$  should be aligned with the cycles of the cosine function not only for the previous analysis to directly apply but also for the FFT coefficients to be applicable. Since the FFT coefficients are the values of DTFT evaluated at frequencies  $\omega = \frac{k\pi}{N}$ ,  $k = 0, \dots, 2N - 1$ , this means  $h_g$  should be  $\frac{k\pi}{N}$  for any integer  $0 \leq k \leq N$ .

For the asymmetrical integrand, since the negative side of the integrand approaches zero faster than the right hand side, we should find end points for both sides. For the positive side, the initial guess

$$x_0^* = \log \left( -\frac{2}{\pi} \left( \log(\epsilon) + \alpha \log \left( \frac{\sin \frac{h_g}{2}}{\sin h_g} \right) \right) \right) \quad (3.22)$$

can be used, where  $x^*$  is similarly defined as  $x^*$  but the ratio is now between the value of the integrand evaluated at the points  $h_g$  and  $\frac{h_g}{2}$ . The initial guess for  $x^*$  (3.11) should also be replaced by

$$x_0^* = \log \left( -\frac{2}{\pi(\alpha + 1)} \left( \log(\epsilon) + \alpha \log \left( \frac{1}{\pi} \sin \frac{h_g}{2} \right) \right) \right). \quad (3.23)$$

Once both  $x^*$  and  $x^*$  are determined, we find a  $N_l$  such that  $\frac{N_l x^*}{N_l} \geq x^*$ . And the negative portion of the summation should terminate at  $-N_l$ .

For the region  $h_g$  to  $\pi$ , the integral is further split into  $N - k_g$  integration regions, where  $k_g = \frac{N}{\pi} h_g$ . In each region, polynomial interpolation is applied to the spectral function. For even polynomial order  $N_f$ , 2 consecutive regions are grouped together so that the interpolation is symmetric over the range of integration. Then, for each region  $m$ ,  $((k_g + 2m)h, (k_g + 2m + 2)h)$ ,  $m = 0, \dots, \frac{N - k_g}{2}$  for even  $N_f$  and  $((k_g + m)h, (k_g + m + 1)h)$ ,  $m = 0, \dots, N - k_g$  for odd  $N_f$ , one wishes to find a set of weights  $\mathbf{b}^{n,m}$ , for  $n = 0, \dots, N$ , such that

$$\int_{(k_g + qm)h}^{(k_g + q(m+1))h} \cos(nx) f(x) dx = \sum_{j=0}^{N_f} f \left( \left( k_g + q(m+1) - 1 + j - \left\lfloor \frac{N_f}{2} \right\rfloor \right) h \right) \mathbf{b}_j^{n,m} + O(h^{N_s}), \quad (3.24)$$

where  $h = \frac{\pi}{N}$ ,  $q = 2$  when  $N_f$  is even and  $q = 1$  when  $N_f$  is odd,  $f$  is analytic within the integration limits including the endpoints, and  $N_s$  is the convergence order to be determined. Replacing  $f$  with a polynomial of order  $N_f$ , the summation exactly equals the integral when  $\mathbf{b}^{n,m}$  satisfies moments up to degree  $N_f$ , that is,

$$\sum_{j=0}^{N_f} \left( \left( k_g + q(m+1) - 1 + j - \left\lfloor \frac{N_f}{2} \right\rfloor \right) h \right)^k \mathbf{b}_j^{n,m} = \int_{(k_g + qm)h}^{(k_g + q(m+1))h} \cos(nx) x^k dx, \quad \text{for } k = 0, \dots, N_f. \quad (3.25)$$

One can shift the integral so that the monomials are 0 at the centre as such

$$h^k \sum_{j=0}^{N_f} \left( j - \frac{N_f}{2} \right)^k \mathbf{b}_j^{n,m} = \int_{-\frac{qh}{2}}^{\frac{qh}{2}} \cos(n(x + c_m)) x^k dx, \quad (3.26)$$

where  $c_m = (k_g + q(m + \frac{1}{2}))h$ . Using the identity  $\cos(x) = \frac{1}{2}(e^{ix} + e^{-ix})$ , we have

$$\mathbf{J}_k^{n,m} = \int_{-\frac{h}{q}}^{\frac{h}{q}} \cos(n(x + c_m)) x^k dx = \frac{i^{k-1}}{2n^{k-1}} \left[ \Gamma(1 + k, -inx) e^{inc_m} - (-1)^k \Gamma(1 + k, inx) e^{-inc_m} \right]_{-\frac{qh}{2}}^{\frac{qh}{2}}. \quad (3.27)$$





which can be substituted into (3.32) to give

$$p(x) = \begin{bmatrix} 1 & x - c_m & \cdots & (x - c_m)^{N_f} \end{bmatrix} \begin{pmatrix} \frac{1}{0!} & & & 0 \\ & \frac{1}{1!} & & \\ & & \ddots & \\ 0 & & & \frac{1}{N_f!} \end{pmatrix} \begin{bmatrix} f(c_m) \\ f'(c_m) \\ \vdots \\ f^{(N_f)}(c_m) \end{bmatrix} + \begin{pmatrix} \begin{bmatrix} 1 & & & 0 \\ & h & & \\ & & \ddots & \\ 0 & & & h^{N_f} \end{bmatrix}^{-1} \begin{bmatrix} 1 & -\frac{N_f}{2} & \cdots & \left(-\frac{N_f}{2}\right)^{N_f} \\ 1 & 1 - \frac{N_f}{2} & \cdots & \left(1 - \frac{N_f}{2}\right)^{N_f} \\ \vdots & \vdots & & \vdots \\ 1 & \frac{N_f}{2} & \cdots & \left(\frac{N_f}{2}\right)^{N_f} \end{bmatrix}^{-1} \begin{bmatrix} \left(-\frac{N_f}{2}\right)^{N_f+1} \\ \left(1 - \frac{N_f}{2}\right)^{N_f+1} \\ \vdots \\ \left(\frac{N_f}{2}\right)^{N_f+1} \end{bmatrix} \frac{h^{N_f+1}}{(N_f+1)!} f^{(N_f+1)}(c_m) + O(h^{N_f+2}) \end{pmatrix}. \quad (3.34)$$

Comparing to the Taylor's polynomial of  $f$  at  $c_m$ , the error starts at  $(N_f + 1)$ -th term. However, using the symmetry of each even row and anti-symmetry of each odd row of the Vandemonde matrix [15], the even degree monomials multiplied by the  $(N_f + 1)$ -th term are eliminated for even  $N_f$ . Further expanding the cosine function about  $c_m$ , and integrating it with the monomials, we find that the local integration error is

$$h^{N_f+1} \int_{-h}^h (C_1 x + C_2 x^2 + \cdots) + O(h^{N_f+2}) dx, \quad (3.35)$$

$$= h^{N_f+1} \int_{-h}^h (C_2 x^2 + C_4 x^4 + \cdots) dx + O(h^{N_f+3}), \quad (3.36)$$

$$= O(h^{N_f+3}), \quad (3.37)$$

where  $C_j$  are bounded constants. Therefore, the global error order is  $N_s = N_f + q$ . Since even order interpolation gives an additional order of convergence rate, it is superior and preferred. However, it does impose an additional restriction on  $h_g$  since  $N - k_g$  must now be even. Note that  $h_g$  cannot be reduced with increase  $N$  or the expansion at  $h_g$  leads to terms  $x^n O(h_g^{\alpha-n})$  which limits convergence to  $O(h^{1+\alpha})$ , which is the same as the trapezoidal rule. Therefore, the number of terms for evaluating the tanh-sinh rule must be doubled for each halving of  $h$ . For the choice of  $N_f$ , it should satisfy  $N_f + q > 2 \max(N_q - n - N_c + 1, N_c) + \alpha$ . For physical problems,  $\alpha$  should be less than 2. Therefore, choosing  $N_f = 2 \max(N_q - n - N_c + 1, N_c)$  is sufficient.

Because nodes outside the integration region are used for interpolation, on the end points, the nodes required may be out of bound of the FFT coefficients but since the DTFT spectrum is cyclic and symmetric about  $\pi$ , one can simply use the mirrored points. The formulation presented here is not standard compared to the Filon-Simpson method where the summation uses only nodes within the integration limits. This approach to integrate a smaller range from the centre of the interpolation produces a smaller error because of the well-known Runge phenomenon of Lagrange interpolation. However, this approach does not allow sparsification of the stencil for higher dimensions as each integration region calls for neighbouring nodes from the previous region. For 2D integration, there is not much saving, compared to directly applying the tensor product on the 1D quadrature weights, as almost half the nodes are still required, but sparsified stencils may be much more efficient for 3D. To compute the weights for integrating over the range of end point nodes, one simply replaces  $\frac{qh}{2}$  with  $\frac{N_f h}{2}$  in (3.28) when computing the moments on the right hand side of (3.31). For sparse nodes, one may either use the Smolyak algorithm described in Subsection 2.3 or solve the system of equations by setting up the moments in a similar way as (2.28).

#### 4. Numerical Experiment

In this section, we test the stencil evaluated for 4th order convergence on two examples and compare the error convergence against stencils evaluated via FFT. Moreover, we test whether increasing the isotropy order of the stencil

by increasing the quadrature order improves the isotropy of the error function as predicted. Both examples are isotropic functions of the radius from the origin. Furthermore, we only consider the 2D problem. This not only allows us to observe the error pattern of the stencil, but the analytical solution of their fractional Laplacian are also easy to find. In the first example, we seek the fractional Laplacian of

$$f_1(r) = \begin{cases} (1-r^2)^\beta & r \leq 1, \\ 0, & \text{otherwise,} \end{cases} \quad (4.1)$$

where  $\beta = 6.6$ . The solution of its fractional Laplacian in 2D is given by

$$-(-\Delta)^{\frac{\alpha}{2}} f_1(r) = \begin{cases} -2^\alpha \frac{\Gamma(1+\beta)\Gamma(1+\frac{\alpha}{2})}{\Gamma(1+\beta-\frac{\alpha}{2})} {}_2F_1\left(1+\frac{\alpha}{2}, \frac{\alpha}{2}-\beta; 1; r^2\right), & r \leq 1, \\ -\frac{2^\alpha}{r^{2+\alpha}} \frac{\Gamma(1+\frac{\alpha}{2})}{(1+\beta)\Gamma(-\frac{\alpha}{2})} {}_2F_1\left(1+\frac{\alpha}{2}, 1+\frac{\alpha}{2}+2+\beta; r^{-2}\right), & r > 1, \end{cases} \quad (4.2)$$

where  ${}_qF_p$  is the generalised hypergeometric function. Here, we define the approximation error as

$$E_i^\alpha = \frac{1}{N_{\max}^2} \sum_{j=-N_{\max}}^{N_{\max}} \sum_{k=-N_{\max}}^{N_{\max}} \left| \Delta^{\frac{\alpha}{2}} f(r_{i,j,k}) - N_i^{-\alpha} \sum_{m=-N_i}^{N_i} \sum_{n=-N_i}^{N_i} \mathbf{H}_{n,m}^\alpha f\left(r_{j+\frac{N_{\max}}{N_i}n, k+\frac{N_{\max}}{N_i}m}\right) \right|, \quad (4.3)$$

where  $N_i = 2^{i+4}$ ,  $N_{\max} = 2^8$ ,  $r_{i,j} = \sqrt{\left(\frac{i}{N_{\max}}\right)^2 + \left(\frac{j}{N_{\max}}\right)^2}$ , and  $\mathbf{H}^\alpha$  is the 2D central difference stencil. Moreover, we define the rate of convergence as

$$r_i^\alpha = \log_2\left(\frac{E_i^\alpha}{E_{i+1}^\alpha}\right). \quad (4.4)$$

Tables 4.1 and 4.2 compare respectively the approximate error and convergence rate of various stencils. Denoted as ‘Sin-FFT’ is the stencil defined as

$$\mathbf{H}_{n,m}^\alpha = -\frac{1}{4N_i^2} \sum_{j=0}^{2N_i-1} \sum_{k=0}^{2N_i-1} \left(4\left(\sin^2\frac{\pi j}{N_i} + \sin^2\frac{\pi k}{N_i}\right)\right)^{\frac{\alpha}{2}} e^{-i2\pi\left(\frac{nj+mk}{N_i}\right)}, \quad (4.5)$$

which is the second order stencil described in [ref], while ‘He-FFT’ and ‘He-Filon’ refer to the stencils defined by (3.3) with  $N_c = 2$  and  $N_q = 4$ . The integral is respectively approximated by FFT, and composite double exponential 4th order Filon method. It can be seen that when the absolute error of solution is small enough so that the error from the approximation the inverse DTFT by FFT dominates, neither ‘Sin-FFT’ nor ‘He-FFT’ converges because FFT causes an  $O(1)$  error as predicted for a function with non-zero DC in the spectrum (a positive function is guaranteed to have DC). In fact, a small negative convergence is observed for ‘Sin-FFT’ possibly due to accumulation of numerical error. When the approximation error is initially large, for example, in the  $\alpha = 1.9$  case, the solution can converge with increasing  $N$ . ‘He-FFT’ converges at the same rate as ‘He-Filon’ initially but the rate quickly diminishes. Similarly for ‘Sin-FFT’, the solution converges at smaller  $N$ , but it slows down once the error is saturated. However, ‘He-Filon’ approaches to the theoretical convergence rate  $2N_c = 4$  as  $N$  increases. This example demonstrates that FFT is insufficient for proper convergence of the solution while higher order integration method solves this problem.

In another example, we attempt to approximate the fractional Laplacian of

$$f_2(r) = \begin{cases} (4r(1-r))^n, & r \leq 1, \\ 0, & \text{otherwise,} \end{cases} \quad (4.6)$$

where  $n$  is set to 6. It has the following solution:

$$-(-\Delta)^{\frac{\alpha}{2}} f_2(r) = \begin{cases} \sqrt{\pi} 2^{n+\alpha} r^{n-\alpha} \left( \frac{\Gamma(\frac{\alpha-1-n}{2})\Gamma(2+n)r}{\Gamma(-\frac{n+1}{2})\Gamma(\frac{\alpha}{2})\Gamma(\frac{3+n-\alpha}{2})} {}_4F_3\left(\frac{1-n}{2}, 1-\frac{n}{2}, \frac{3+n}{2}, \frac{3+n}{2}; \frac{3}{2}, \frac{3+n-\alpha}{2}, \frac{3+n-\alpha}{2}; r^2\right) \right. \\ \quad \left. - \frac{\Gamma(\frac{\alpha-n}{2})\Gamma(1+n)}{\Gamma(-\frac{n}{2})\Gamma(\frac{1+n}{2})\Gamma(\frac{2+n-\alpha}{2})} {}_4F_3\left(-\frac{n}{2}, \frac{1-n}{2}, \frac{2+n}{2}, \frac{2+n}{2}; \frac{1}{2}, 1+\frac{n-\alpha}{2}, 1+\frac{n-\alpha}{2}; r^2\right) \right) \\ \quad - \frac{2^{1+2n+\alpha}\Gamma(\frac{\alpha}{2})\Gamma(1+n)\Gamma(1+\frac{\alpha}{2})}{\Gamma(1+2n-\alpha)\Gamma(-\frac{\alpha}{2})} {}_4F_3\left(\frac{\alpha}{2}-n, \frac{1+\alpha}{2}-n, 1+\frac{\alpha}{2}, 1+\frac{\alpha}{2}; 1, \frac{1+\alpha-n}{2}, 1+\frac{\alpha-n}{2}; r^2\right), & r \leq 1, \\ -\sqrt{\pi} \frac{2^{\alpha-1}\Gamma(1+n)\Gamma(1+\frac{\alpha}{2})}{r^{2+\alpha}\Gamma(\frac{3}{2}+n)\Gamma(-\frac{\alpha}{2})} {}_4F_3\left(1+\frac{n}{2}, \frac{3+n}{2}, 1+\frac{\alpha}{2}, 1+\frac{\alpha}{2}; 1, \frac{3}{2}+n, 2+n; r^{-2}\right), & r > 1. \end{cases} \quad (4.7)$$

$i$	Sin-FFT	He-FFT	He-Filon	Sin-FFT	He-FFT	He-Filon
	$\alpha=0.1$			$\alpha=0.8$		
0	0.02381	0.01803	0.0001463	0.01241	0.01275	0.004889
1	0.02381	0.01762	1.108e-05	0.01246	0.01251	0.0003958
2	0.02381	0.01717	7.343e-07	0.01250	0.01251	2.678e-05
3	0.02381	0.01670	4.666e-08	0.01251	0.01251	1.712e-06
4	0.02381	0.01618	2.929e-09	0.01251	0.01251	1.076e-07
	$\alpha=1.2$			$\alpha=1.9$		
0	0.01849	0.01996	0.01712	0.1026	0.1227	0.1228
1	0.008014	0.007537	0.001432	0.02641	0.01096	0.01099
2	0.007499	0.007526	9.807e-05	0.006879	0.001041	0.0007705
3	0.007519	0.007525	6.289e-06	0.001988	0.0007552	4.971e-05
4	0.007523	0.007525	3.957e-07	0.0008402	0.0007552	3.132e-06

Table 4.1: Error  $E_i^\alpha$  of the approximation of the fractional Laplacian of (4.1)

$i$	Sin-FFT	He-FFT	He-Filon	Sin-FFT	He-FFT	He-Filon
	$\alpha=0.1$			$\alpha=0.8$		
0	-0.000236	0.0336	3.72	-0.00630	0.0275	3.63
1	-5.92e-05	0.0369	3.92	-0.00391	0.000332	3.89
2	-1.48e-05	0.0406	3.98	-0.000976	6.01e-05	3.97
3	-3.70e-06	0.0448	3.99	-0.000244	7.45e-05	3.99
	$\alpha=1.2$			$\alpha=1.9$		
0	1.21	1.40	3.58	1.96	3.48	3.48
1	0.0958	0.00213	3.87	1.94	3.40	3.83
2	-0.00375	0.000116	3.96	1.79	0.463	3.95
3	-0.000936	8.02e-06	3.99	1.24	0.000119	3.99

Table 4.2: Rate of convergence  $r_i^\alpha$  for (4.1)

$i$	Sin-FFT	He-FFT	He-Filon	Sin-FFT	He-FFT	He-Filon
	$\alpha=0.1$			$\alpha=0.8$		
0	0.06178	0.04680	0.001637	0.05065	0.08479	0.07395
1	0.06179	0.04574	0.0001630	0.03263	0.03290	0.008248
2	0.06180	0.04458	1.200e-05	0.03280	0.03286	0.0006340
3	0.06180	0.04335	7.878e-07	0.03284	0.03285	4.230e-05
4	0.06180	0.04202	4.990e-08	0.03285	0.03285	2.694e-06
	$\alpha=1.2$			$\alpha=1.9$		
0	0.1641	0.3060	0.3022	1.484	2.815	2.816
1	0.04761	0.04281	0.03623	0.3957	0.3877	0.3879
2	0.02090	0.01996	0.002868	0.1010	0.03283	0.03268
3	0.01991	0.01995	0.0001935	0.02588	0.002914	0.002261
4	0.01994	0.01995	1.236e-05	0.007044	0.002041	0.0001456

Table 4.3: Error  $E_i^\alpha$  of the approximation of the fractional Laplacian of (4.6)

$i$	Sin-FFT	He-FFT	He-Filon	Sin-FFT	He-FFT	He-Filon
	$\alpha=0.1$			$\alpha=0.8$		
0	-0.000280	0.0333	3.33	0.634	1.37	3.16
1	-7.00e-05	0.0368	3.76	-0.00755	0.00185	3.70
2	-1.75e-05	0.0405	3.93	-0.00188	0.000165	3.91
3	-4.38e-06	0.0448	3.98	-0.000469	7.97e-05	3.97
	$\alpha=1.2$			$\alpha=1.9$		
0	1.79	2.84	3.06	1.91	2.86	2.86
1	1.19	1.10	3.66	1.97	3.56	3.57
2	0.0705	0.00109	3.89	1.96	3.49	3.85
3	-0.00222	6.09e-05	3.97	1.88	0.514	3.96

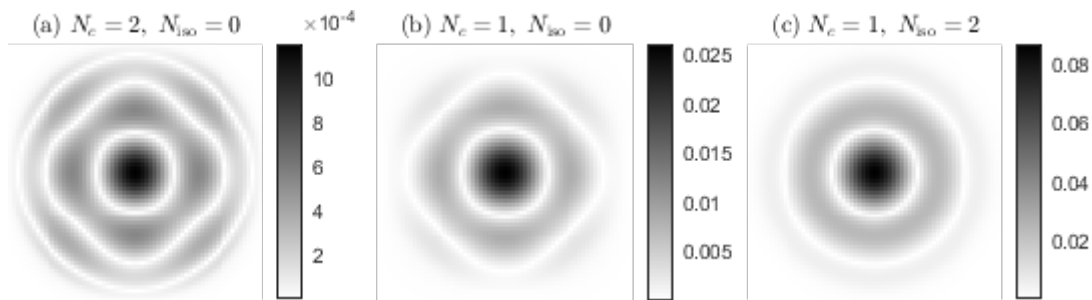
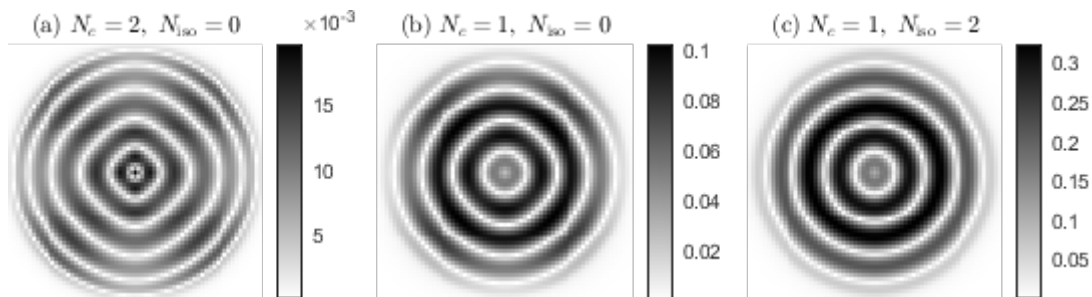
Table 4.4: Rate of convergence  $r_i^\alpha$  for (4.6)

Tables 4.3 and 4.4 list the errors and convergence rates respectively for the approximation of fractional Laplacian of (4.6). Again we observe similar behaviours from each of the stencils. The consistency displayed here follows from the previous analysis.

Other than the convergence of solution, another aspect worth looking into is the isotropy of the stencil. From (2.15), the combination of  $N_c = 2$  and  $N_q = 4$  does not lead to isotropic error terms. Let  $N_{\text{iso}} = N_q - n - N_c + 1$ , we compare the stencil evaluated with  $N_{\text{iso}} = 2$  against those evaluated with  $N_{\text{iso}} = 0$  in order to verify the improved isotropy of the solution. Figures 4.1 and 4.2 illustrate, respectively for  $f = f_1$  and  $f = f_2$ , the absolute error defined by

$$\left| \Delta^{\frac{\alpha}{2}} f(r_{j,k}) - N^{-\alpha} \sum_{m=-N}^N \sum_{n=-N}^N \mathbf{H}_{n,m}^\alpha f(r_{j+n,k+m}) \right|, \quad (4.8)$$

where  $N = 64$ ,  $r_{j,k} = \sqrt{\left(\frac{j}{N}\right)^2 + \left(\frac{k}{N}\right)^2}$ , for  $j, k = -N, \dots, N$ . With  $N_{\text{iso}} = 2$ , the highest order isotropic error term should be 4-th order. This is reflected in both of the plots, where the error pattern is significantly more circular than those of stencils with  $N_{\text{iso}} = 0$ . This verifies the error analysis that the isotropy of the error transfers to the fractional order stencil. However, this comes at the cost of higher absolute error when even compared to the stencil with the same error order. In practice, for diffusion or wave propagation applications, this isotropy may be preferred over reduced error.

Figure 4.1: Error pattern from approximating fractional Laplacian of (4.1) with  $N = 64$ Figure 4.2: Error pattern from approximating fractional Laplacian of (4.6)  $N = 64$ 

## 5. Conclusion

In conclusion, the differentiation problem of Laplacian has been turned into multiple integral problems, which requires the application of multiple quadrature rules, namely the Hermite Gauss quadrature and quadrature for equidistant nodes, tanh-sinh double exponential substitution trapezoidal quadrature, and Filon quadrature. By applying the composite tanh-sinh, and Filon quadrature method, the issue with FFT preventing the convergence of the solution has been successfully resolved. Moreover, this method of obtaining higher order stencil is significantly more efficient than methods presented in [6, 15] because the linear combination is applied in the finite space of integer order stencil. Additionally, the choice of Hermite polynomials allows us to generate stencils with Gaussian error terms, which are isotropic. Error isotropy may be more important than absolute error in physical problems where propagation directions are of great significance.

While we have reviewed in details regarding the lattice Boltzmann method, including the generalisation to higher order convergence and exact solutions for 2D stencils, the mystery of the possibility of the odd order quadrature being able to integrate 1 higher order polynomial with the appropriate scaling factor for the space variable remains. Perhaps a future study into the existence of roots of the polynomial (2.26) is worthwhile. Another potential future study from a mathematical standpoint is a more rigorous analysis for the convergence of double exponential rule for finite oscillatory integrals.

## References

- [1] B. E. Treeby, B. T. Cox, Modeling power law absorption and dispersion for acoustic propagation using the fractional Laplacian 127 (5) 2741–2748. doi:10.1121/1.3377056. URL <http://asa.scitation.org/doi/10.1121/1.3377056>
- [2] S. Holm, S. P. N asholm, Comparison of fractional wave equations for power law attenuation in ultrasound and elastography 40 (4) 695–703. doi:10.1016/j.ultrasmedbio.2013.09.033. URL <http://www.sciencedirect.com/science/article/pii/S0301562913010685>
- [3] A. de Pablo, F. Quir os, A. Rodr iguez, J. L. V azquez, A fractional porous medium equation 226 (2) 1378–1409. doi:10.1016/j.aim.2010.07.017. URL <https://linkinghub.elsevier.com/retrieve/pii/S0001870810003130>

- [4] V. A. Volpert, Y. Nec, A. A. Nepomnyashchy, *Fronts in anomalous diffusion-reaction systems* 371 (1982) 20120179. doi:10.1098/rsta.2012.0179.  
URL <https://royalsocietypublishing.org/doi/10.1098/rsta.2012.0179>
- [5] A. Lischke, G. Pang, M. Gulian, F. Song, C. Glusa, X. Zheng, Z. Mao, W. Cai, M. M. Meerschaert, M. Ainsworth, G. E. Karniadakis, What is the fractional Laplacian? a comparative review with new results 404 109009. doi:10.1016/j.jcp.2019.109009.  
URL <https://linkinghub.elsevier.com/retrieve/pii/S0021999119307156>
- [6] Z. Hao, Z. Zhang, R. Du, Fractional centered difference scheme for high-dimensional integral fractional Laplacian 424 109851. doi:10.1016/j.jcp.2020.109851.  
URL <https://linkinghub.elsevier.com/retrieve/pii/S0021999120306252>
- [7] M. Ilic, F. Liu, I. Turner, V. Anh, Numerical approximation of a fractional-in-space diffusion equation, i 8 (3) 19.
- [8] K. K. Mattila, L. A. Hegele Júnior, P. C. Philippi, High-accuracy approximation of high-rank derivatives: isotropic finite differences based on lattice-Boltzmann stencils 2014 1–16. doi:10.1155/2014/142907.  
URL <http://www.hindawi.com/journals/tswj/2014/142907/>
- [9] P. C. Philippi, L. A. Hegele, L. O. E. dos Santos, R. Surmas, From the continuous to the lattice Boltzmann equation: The discretization problem and thermal models 73 (5) 056702. doi:10.1103/PhysRevE.73.056702.  
URL <https://link.aps.org/doi/10.1103/PhysRevE.73.056702>
- [10] F. Qi, B.-N. Guo, Some properties of the Hermite polynomials 28 (6) 925–935. doi:10.1515/gmj-2020-2088.  
URL <https://www.degruyter.com/document/doi/10.1515/gmj-2020-2088/html>
- [11] A. R. Krommer, C. W. Ueberhuber, *Computational Integration*, Society for Industrial and Applied Mathematics. doi:10.1137/1.9781611971460.  
URL <http://epubs.siam.org/doi/book/10.1137/1.9781611971460>
- [12] G. H. Golub, J. H. Welsch, Calculation of Gauss quadrature rules 23 (106) 221–221. doi:10.1090/S0025-5718-69-99647-1.  
URL <http://www.ams.org/jourcgi/jour-getitem?pii=S0025-5718-69-99647-1>
- [13] T. Gerstner, M. Griebel, Numerical integration using sparse grids 18 (3) 209–232. doi:10.1023/A:1019129717644.  
URL <http://link.springer.com/10.1023/A:1019129717644>
- [14] M. McKiernan, On the  $n$ th derivative of composite functions 63 (5) 331. doi:10.2307/2310518.  
URL <http://www.jstor.org/stable/2310518?origin=crossref>
- [15] P. H. Lam, H. C. So, C. F. Chan, Arbitrary order of convergence for riesz fractional derivative via central difference method. arXiv:2108.03772.  
URL <http://arxiv.org/abs/2108.03772>
- [16] S. Haber, The tanh rule for numerical integration 14 (4) 668–685. doi:10.1137/0714045.  
URL <http://epubs.siam.org/doi/10.1137/0714045>
- [17] M. Mori, M. Sugihara, The double-exponential transformation in numerical analysis 127 (1) 287–296. doi:10.1016/S0377-0427(00)00501-X.  
URL <https://linkinghub.elsevier.com/retrieve/pii/S037704270000501X>
- [18] G. Beylkin, L. Monz'ón, Approximation by exponential sums revisited 28 (2) 131–149. doi:10.1016/j.acha.2009.08.011.  
URL <http://www.sciencedirect.com/science/article/pii/S1063520309000906>
- [19] E. O. Tuck, A simple "Filon-trapezoidal" rule 21 (98) 239. doi:10.2307/2004168.  
URL <https://www.jstor.org/stable/2004168?origin=crossref>